

Experimental Observation of Ion Hose Instability

K. J. O'Brien, G. W. Kamin, T. R. Lockner, J. S. Wagner, I. R. Shokair, P. D. Kiekel, I. Molina, D. J. Armistead, S. Hogeland,^(a) E. T. Powell,^(b) and R. J. Lipinski

Sandia National Laboratories, Albuquerque, New Mexico 87185

(Received 3 November 1987)

A theoretically predicted instability of the ion-focus-regime guiding of intense relativistic electron beams, known as the ion hose instability, has been observed in an experiment. A 1.5- μ s, 1.2-kA, 2.2-MeV electron beam has been successfully injected into and propagated down a 21-m preionized channel. Off-axis beam oscillations have been found to grow and then saturate at large amplitude. Observed growth times, real frequencies, and saturated amplitudes are in agreement with theoretical scaling predictions and with numerical simulation of the ion hose instability.

PACS numbers: 41.80.Ee, 52.35.-g, 52.40.Mj

Ion-focus-regime (IFR) guiding of intense electron beams has emerged in recent years as an effective electron-beam transport technique.^{1,2} When an electron beam is injected into a plasma column, the beam head radially expels plasma electrons. The resulting positive-ion column provides an electrostatic guide force for the remainder of the beam. The experimental and theoretical work reported in this Letter was carried out to detect and investigate a potential disruption of IFR guiding known as the "ion hose" instability.^{3,4}

Ion hose instability develops when an offset between an electron beam and IFR channel causes mutual transverse oscillations in response to the electrostatic guide force. The key physical parameter, characterizing the strength of the guide force, is the neutralization fraction $f = N_i/N_e$, where N_i is the line density of channel ions (singly charged) and N_e is the beam line density. Previous attempts at detecting ion hose instability were hampered by an inability to assure that f was not continually modified, as a function of time into the beam pulse, by beam-generated ionization.^{5,6}

The characteristic transverse oscillation wavelength of an electron beam is $\lambda_{\beta e} = 2\pi c/\Omega_{\beta e}$, where $\Omega_{\beta e}$ is the be-

atron frequency $\Omega_{\beta e} = (c/a)(fI_b/\gamma I_A)^{1/2}$ [c is the speed of light; γ , the relativistic γ ; $I_A = m_e c^3/e$ the Alfvén current; I_b , beam current; $a^2 = (a_e^2 + a_i^2)/2$ with a_e and a_i the beam and channel scale radii (cgs Gaussian units)]. The characteristic transverse oscillation frequency of an IFR channel is $\omega_{\beta i} = (\gamma m_e/f m_i)^{1/2} \Omega_{\beta e}$.

In the limit of an immobile channel ($\omega_{\beta i} = 0$), the ion hose frequency is $\omega = 0$ and the beam responds with wavelength $\lambda = \lambda_{\beta e}$ precisely. A mobile channel ($\omega_{\beta i} \neq 0$) responds to the beam motion so that $\omega \neq 0$, but the ion hose wavelength is still $\lambda \approx \lambda_{\beta e}$ since $(\gamma m_e/m_i)^{1/2} \ll 1$. The IFR channel is imprinted with a modulation at $\lambda \approx \lambda_{\beta e}$ and succeeding portions of beam are therefore driven at a frequency close to $\Omega_{\beta e}$. This resonant interaction increases the amplitude of beam motion as a function of propagation distance. Being a convective instability, the amplitude also increases from head to tail on the beam.

Buchanan has used nonlinear equations to describe the mutual electrostatic interaction of an overlapping electron beam and IFR channel, each with Gaussian radial profile.⁴ We have augmented his equations to include the effect of the weak axial magnetic field which is present in our experiment. Our model equations are

$$\frac{\partial^2 \mathbf{b}}{\partial z^2} = -2a^2 k_{\beta e}^2 \frac{\mathbf{b} - \mathbf{c}}{(\mathbf{b} - \mathbf{c})^2} (1 - e^{-(\mathbf{b} - \mathbf{c})^2/2a^2}) + k_{ce} \hat{\mathbf{z}} \times \frac{\partial \mathbf{b}}{\partial z}, \quad (1)$$

$$\frac{\partial^2 \mathbf{c}}{\partial \xi^2} = -2a^2 k_{\beta i}^2 \frac{\mathbf{c} - \mathbf{b}}{(\mathbf{b} - \mathbf{c})^2} (1 - e^{-(\mathbf{b} - \mathbf{c})^2/2a^2}) - k_{ci} \hat{\mathbf{z}} \times \frac{\partial \mathbf{c}}{\partial \xi}. \quad (2)$$

In these equations $\mathbf{b} = (b_x, b_y)$ and $\mathbf{c} = (c_x, c_y)$ are offsets of beam and channel. Cyclotron wave numbers are $k_{ce} = 2\pi eB/\gamma m_e c^2$ and $k_{ci} = (\gamma m_e/m_i) k_{ce}$; B is the applied axial magnetic field. Betatron wave numbers are $k_{\beta e} = \Omega_{\beta e}/c$ and $k_{\beta i} = \omega_{\beta i}/c$. $\hat{\mathbf{z}}$ is a unit vector in the direction of beam propagation. $\xi = ct - z$, and t is time in the laboratory reference frame. We use a saddle-point approximation for the linearization of Eqs. (1) and (2) which is valid in the limit where $zk_{\beta e} \gg \xi k_{\beta i}$.⁷ Our result for the magnitude of the offset may be written as

$$b(z, \xi) = b_0 e^{G(z, \xi)}, \text{ where}$$

$$G(z, \xi) = (3^{3/2}/8) (k_{\beta i}^2 \xi^2 k_{\beta e} z)^{1/3} (1 + \Omega_{ce}^2/4\Omega_{\beta e}^2)^{-1/6} \quad (3)$$

is the logarithmic gain and $\Omega_{ce} = ck_{ce}$. In the limit $\Omega_{ce} \rightarrow 0$, this recovers Buchanan's result.⁴ In the experiment, $\Omega_{ce}^2/4\Omega_{\beta e}^2 \ll 1$. The saddle-point result provides scaling predictions used to interpret the experimental data. The electron beam in the TROLL accelerator^{8,9} is

created in a shielded cathode, but then enters a solenoidal magnetic field and begins to spin because of conservation of canonical momentum P_θ . The spin effect is not described by the preceding analysis. This spin frequency is calculated to be $\nu \approx 15$ MHz, but the "spin" is not thought to couple to the "orbital" motion of the offset beam.

In order to search for the predicted instability, an experiment was conducted at Sandia National Laboratories (Fig. 1). A long-pulse accelerator, TROLL, was developed^{8,9} which produced a 1.5- μ s, 1.2-kA electron beam with a 2.2-MeV voltage plateau for this experiment. The 11-cm-diam beam was focused down to 2 cm with a solenoid lens and injected into a preformed plasma channel. The plasma channel was generated by means of a hot-filament electron source immersed in a weak cusp magnetic field. The field in the downstream end of the cusp was matched to a 60-G axial field in the gas-filled propagation tank so that the plasma generated in the cusp region diffused along the field lines to the end of the tank. The line density N_i of channel ions was found to be proportional to the power supplied to the electron source. The tank was pumped to a base pressure below 6×10^{-6} Torr, thus assuring negligible contamination of the noble-gas plasma. The whole system was backfilled with noble gas to 3×10^{-5} Torr, measured in the tank with an ionization gauge. Helium, argon, and xenon gas were individually used in order to ensure a monatomic ion species and to provide a significant dynamical range in ion mass.

Ion-channel profile and density measurements were made with Langmuir probes. The profile was found to be nearly Gaussian with $1/e$ radius $a_i \approx 2.0$ cm. The density measurements were used to compute the values of f . To avoid beam perturbations no channel measurements were made during the beam shots. Beam diagnostics consisted of diode voltage and current measurements, and B -dot loops at 0, 6.6, and 19 m down the tank (Fig. 1). At the 6.6- and 19-m locations, four B -dot loops were positioned 90° apart to locate the centroid of

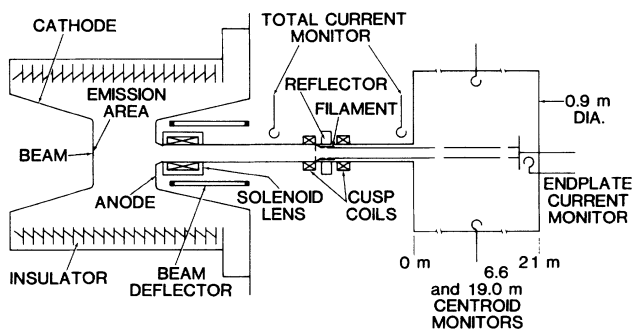


FIG. 1. Schematic of experimental setup showing TROLL diode, solenoidal lens, channel formation section, and gas-filled tank.

the beam current. The current-normalized position signals were calibrated with an offset transmission line running the length of the drift chamber and driven by a fast pulser. A 3.8-cm-radius current collector was positioned in the center of the end flange of the tank at 21 m. This monitor was used with the position monitors at 6.6 and 19 m to confirm the beam displacement, to determine the approximate beam diameter, and to center the channel. An x-ray pinhole camera was used to determine the time-integrated beam position and diameter on each shot. Time-dependent beam position and diameter were monitored on each shot with a four-frame x-ray framing camera.

In order to investigate beam transport without a focusing channel, and to measure the initial conditions, shots were fired with the tank field off and the cusp coils and focusing magnet on. X-ray photographs of the beam incident on a target at $z=0$ showed a 1.3-cm offset in the x direction and a $1/e$ radius $a_e \approx 1.2$ cm. A pulse-length-averaged initial transverse beam velocity $(v_x, v_y) = (0.6, 0.1)$ cm/ns was deduced from the 6.6-m centroid monitor. There was no visible x-ray image at 21 m and no measurable current collected. This indicated free expansion of the beam.

With the tank field on, but no focusing channel, a diffuse x-ray image was seen on the end flange with 200 A of collected current. If the beam had collisionally ionized the gas, thereby slightly increasing f above zero, an improved focus as a function of time into the pulse would have been apparent. The collected current did not show such an improvement in focus with time.

The change δn_i in ion density n_i over the pulse duration τ_p due to ionization by the beam is $\delta n_i = n_e n_n \tau_p \sigma_{en} C$

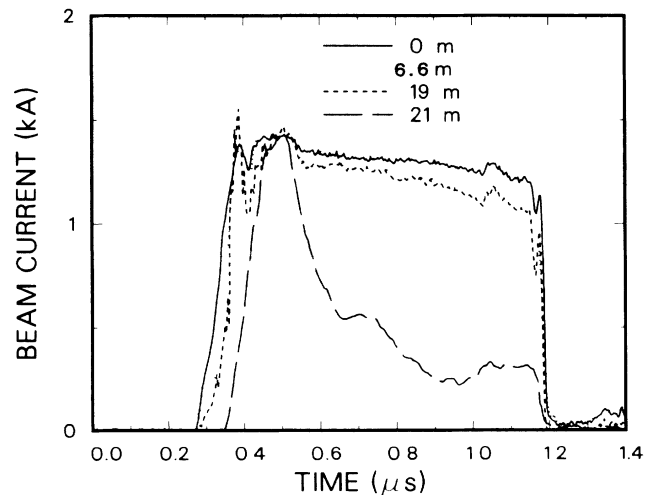


FIG. 2. Beam current vs time at various locations downstream for a Xe shot. At 0, 6.6, and 19 m, the current is that enclosed within the 40-cm-radius tank. At 21 m the current is that collected on a 3.8-cm-radius collector. The 21-m trace shows drastic loss of the beam tail due to ion hose instability.

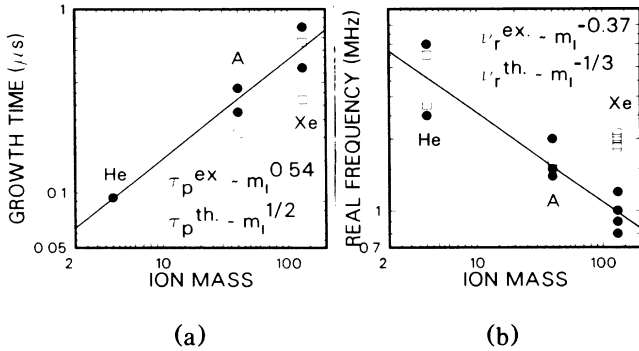


FIG. 3. Growth time and real frequency vs IFR channel ion mass m_i . Shown are the data (solid symbols), simulation (open symbols), and theoretical predictions.

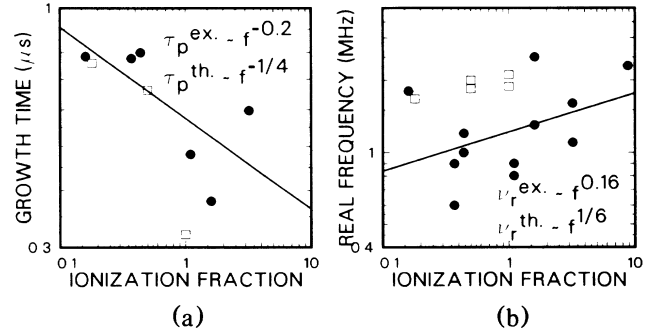


FIG. 4. Growth time and real frequency vs IFR channel neutralization fraction $f = N_i/N_e$. Shown are the data (solid symbols), simulation (open symbols), and theoretical predictions.

(n_n , neutral-gas density; σ_{en} , electron-neutral ionization cross section). For our experiment $n_n \approx 10^{12} \text{ cm}^{-3}$; $n_e \approx 10^{10} \text{ cm}^{-3}$; $\tau_p \approx 10^{-6} \text{ s}$; $\sigma_{en} \approx 10^{-18} \text{ cm}^2$; therefore $\delta n_i/n_i \approx 10^{-2}$. In order for $\delta n_i/n_i \approx 1$ the beam would have to pinch down radially by a factor of 10. The four-frame x-ray framing camera showed no evidence of such pinching. Secondary ionization by the ions is unimportant since $v_i/c \sim (1-f)^{1/2}[(60 \text{ keV})/m_i c^2]^{1/2} \approx 10^{-2}$ (v_i ion radial velocity); therefore, assuming $\sigma_{in} \approx 10^{-16} \text{ cm}^2$, we have $\delta n_i/n_i \sim n_n \tau_p \sigma_{in} v_i \approx 10^{-2}$.¹⁰

In order to investigate ion hose, two key parameters were varied, with all others held fixed. First, f was changed by means of variation of N_i ; second, ion mass m_i was varied. To see gain G at a given point z in the laboratory pulse length $\tau_p \sim (z k_{pe})^{-1/2} \omega_{\beta i}^{-1}$ must propagate past the point. The predicted scaling of τ_p with f and m_i is thus $\tau_p \sim f^{-1/4} m_i^{1/2}$. At a location z in the laboratory the gain of a segment of beam, with respect to the amplitude at $\xi=0$, scales with f and m_i as $G \sim f^{1/6} m_i^{-1/3}$; in particular, the amplitude at the end of the beam pulse thus scales as $f^{1/6} m_i^{-1/3}$. The frequency ω_r of oscillations observed as the beam streams past a location z in the laboratory is also predicted to scale as $\omega_r \sim f^{1/6} m_i^{-1/3}$ with f and m_i .

Figure 2 shows the total current within the tank measured at 0, 6.6, and 19 m, as well as the current collected on the 3.8-cm collector at 21 m, for a Xe shot. These data show that all of the beam was transported within the tank diameter but only the head of the beam was transported within a 3.8-cm radius. The loss of the tail of the beam is consistent with ion hose instability: Coherent transverse oscillations are phase-mixed and converted into a head-to-tail radius and emittance growth. This interpretation is supported by the four-frame x-ray framing camera which showed evidence of a monotonic increase in beam radius from head to tail.

Figure 3(a) depicts $\log \tau_p$ for gain $G = \log(4.0/1.3)$ plotted as a function of $\log m_i$ for gases He, A, and Xe. The values of f for the shots depicted fall within the range 0.44 to 1.1. The best-fit line has slope 0.54 ± 0.08

which agrees well with the predicted slope of $\frac{1}{2}$. Figure 3(b) shows the logarithm of the real frequency $\nu_r = \omega_r/2\pi$ of oscillations observed at 6.6 m as a function of $\log m_i$. The range of f values is the same as in Fig. 3(a). The best-fit line has slope -0.37 ± 0.06 , which compares well with the predicted slope $-\frac{1}{3}$. In Fig. 4(a) $\log \tau_p$ for gain $G = \log(4.0/1.3)$ as a function of $\log f$ is shown for a Xe channel. The best fit to the data gives a slope of -0.2 ± 0.1 and the theoretical prediction is $-\frac{1}{4}$. Figure 4(b) shows $\log \nu_r$ plotted versus $\log f$ for a Xe channel. Theory predicts a slope of $\frac{1}{6}$ and the best-fit slope is 0.16 ± 0.11 ; the data have a large scatter. Figure 5(a) shows the logarithm of the percentage of charge transported to the 3.8-cm-radius current collector at 21 m plotted versus $\log m_i$. The indicated scaling with m_i is seen to be roughly $m_i^{1/2}$. Figure 5(b) depicts the offset amplitude of one of the more striking argon shots. This shot clearly displays a well-defined wave structure with a growing envelope as expected for ion hose instability.

Computer simulations, using the nonlinear ion hose

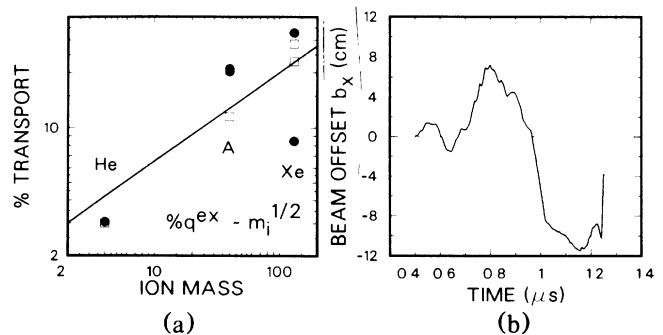


FIG. 5. (a) Percentage of beam charge collected on the 3.8-cm collector at the tank end flange. Shown are the data (solid symbols) and simulation (open symbols). (b) A striking argon shot showing well-defined oscillation and growing envelope of ion hose instability. The data were recorded by the B-dot monitor at the 6.6-m location.

code BUCKSHOT, provide further support for our interpretation of the experiment. BUCKSHOT is a 3D particle code designed to study IFR physics issues.¹¹ The code has been carefully tested by comparison with linear theory and with a numerical solution of Eqs. (1) and (2) without magnetic field for a single beam and channel particle.¹² Initial conditions used in the simulations were chosen to represent the experimentally measured conditions, described earlier, as closely as possible. Code predictions of the scaling of τ_p and ν_r with m_i and f are shown on the plots of the data. The agreement between the nonlinear simulations and the linear theory proves that the linear scaling relations are valid even for large amplitudes.

In conclusion, an experiment was conducted to investigate a transverse instability in an intense electron beam propagating with IFR guiding. The correlation between experiment, linear theory, and nonlinear simulation provides strong evidence that the observed instability is in fact the ion hose instability.

We wish to thank R. Bruce Miller for his advice and encouragement during the course of this work. We also wish to acknowledge useful conversations with Barry Newberger concerning ion hose physics. This work was supported by the U.S. Department of Energy under Contract No. DE-AC04-76-DP00789.

^(a)Permanent address: KTECH, Inc., Albuquerque, NM 87110.

^(b)Permanent address: Princeton Plasma Physics Laboratory, Princeton, NJ 08544.

¹W. E. Martin, G. J. Caporaso, W. M. Fawley, D. Prosnitz, and A. G. Cole, Phys. Rev. Lett. **54**, 685 (1985).

²C. A. Frost, S. L. Shope, R. B. Miller, G. T. Leifeste, C. E. Crist, and W. W. Reinstra, IEEE Trans. Nucl. Sci. **32**, 2754 (1985).

³G. I. Budker, Sov. At. Energy, **1**, 673 (1956).

⁴H. L. Buchanan, Phys. Fluids **30**, 221 (1987).

⁵E. J. Lauer, G. J. Caporaso, Y. P. Chong, D. S. Prono, F. Rainer, K. W. Struve, and J. T. Weir, in Proceedings of the Sixth International Conference on High-Power Particle Beams, Osaka, Japan, 1986 (to be published), p. 746.

⁶R. F. Schneider and J. R. Smith, Phys. Fluids **29**, 3917 (1986); K. T. Nguyen, R. F. Schneider, J. R. Smith, and H. S. Uhm, Appl. Phys. Lett. **50**, 239 (1987).

⁷K. J. O'Brien, unpublished.

⁸A. H. Bushnell, Y. G. Chen, and J. Shannon, in Proceedings of the Sixth Institute of Electrical and Electronics Engineers Pulsed Power Conference, Washington DC, 1987 (to be published).

⁹R. S. Clark, M. T. Buttram, J. W. Poukey, and T. R. Lockner, in Ref. 8.

¹⁰F. F. Rieke and W. Prepejchal, Phys. Rev. A **6**, 4, 1507 (1972).

¹¹J. S. Wagner, unpublished.

¹²I. R. Shokair and J. S. Wagner, unpublished.

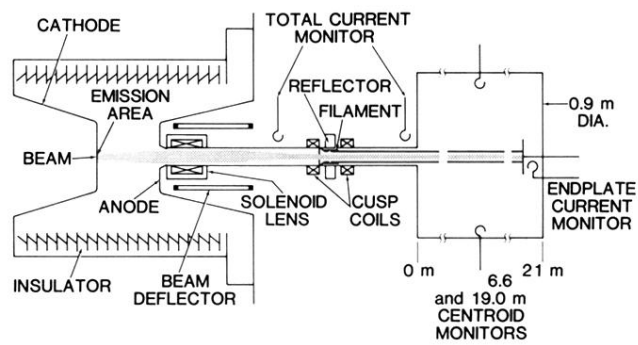


FIG. 1. Schematic of experimental setup showing TROLL diode, solenoidal lens, channel formation section, and gas-filled tank.